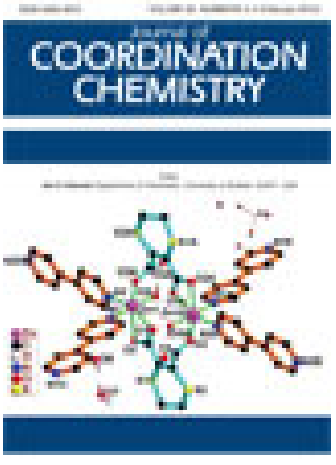

Journal of Coordination Chemistry
Publication details, including instructions for authors and subscription information:
http://www.tandfonline.com/loi/gcoo20

Studies on reactions of some ruthenium sulfoxide bipyridyl complexes with 1,4-bis(salicylidene)phenylenediamine ligand used as spacer

Satyendra N. Shukla [a], Pratiksha Gaur [a], Archana Dubey [a], Sheela Mathews [a] & Ripul Mehrotra [a]
[a] Coordination Chemistry Research Lab, Department of Chemistry, Govt. Model Science College, Jabalpur 482 001, Madhya Pradesh, India
Published online: 03 Feb 2012.

To cite this article: Satyendra N. Shukla, Pratiksha Gaur, Archana Dubey, Sheela Mathews & Ripul Mehrotra (2012) Studies on reactions of some ruthenium sulfoxide bipyridyl complexes with 1,4-bis(salicylidene)phenylenediamine ligand used as spacer, Journal of Coordination Chemistry, 65:4, 602-615, DOI: 10.1080/00958972.2012.657630

To link to this article: http://dx.doi.org/10.1080/00958972.2012.657630

Journal of Coordination Chemistry
Vol. 65, No. 4, 20 February 2012, 602–615

Studies on reactions of some ruthenium sulfoxide bipyridyl complexes with 1,4-bis(salicylidene)phenylenediamine ligand used as spacer

SATYENDRA N. SHUKLA*, PRATIKSHA GAUR, ARCHANA DUBEY, SHEELA MATHEWS and RIPUL MEHROTRA†

Coordination Chemistry Research Lab, Department of Chemistry, Govt. Model Science College, Jabalpur 482 001, Madhya Pradesh, India

(*Received 13 May 2011; in final form 14 December 2011*)

A dinucleating spacer 1,4-bis(salicylidene)phenylenediamine (SALPHEN) derived from 1,4-phenylenediamine and salicylaldehyde has been synthesized and characterized. The ruthenium(II) sulfoxide derivative of 2,2′-bipyridine or 1,10-phenanthroline on reaction with this ligand resulted in the formation of eight dinuclear complexes, which were characterized by elemental analyses, conductivity measurements, magnetic susceptibility, FT-IR, fast atom bombardment-mass spectra, electronic spectroscopy, ^{1}H-NMR, ^{13}C{^{1}H}-NMR, and ^{2}D-NMR spectra (HETCOR). The prepared complexes have two different formulations, [{*trans*-$RuCl_2$(so)(N–N')}$_2$(μ-SALPHEN)] and [{*cis*-$RuCl_2$(so)(N–N')}$_2$(μ-SALPHEN)], where so = dimethyl sulfoxide (DMSO)/tetramethylene sulfoxide (TMSO), N–N' = 2,2′-bipyridine/1,10-phenanthroline, and SALPHEN = 1,4-bis(salicylidene)phenylenediamine. Two moles of ruthenium sulfoxide bipyridine precursor were coordinated to the bidentate SALPHEN through nitrogen. All the complexes possess antibacterial activity against *Escherichia coli* in comparison to Chloramphenicol.

Keywords: Phenyldiamine; 1,4-Bis(salicylidene)phenylenediamine; Ruthenium sulfoxide; Bipyridine

1. Introduction

Development of ruthenium(II/III) dimethyl sulfoxide and tetramethylene sulfoxide complexes as antitumor agents has been established. Ruthenium-based drugs appear to be good alternatives to platinum drugs as they generally exhibit lower toxicity than their platinum counterparts. This has been ascribed to two main reasons: (1) the accumulation of ruthenium compounds in tumors due to the ability of ruthenium to mimic iron in binding to transferrin and (2) the well-accepted phenomenon of "activation by reduction" for Ru(III) → Ru(II) *in vivo*, which is favored in the hypoxic environment of a tumor [1]. Two ruthenium compounds, NAMI-A and KP1019, have already completed phase one clinical trials as anticancer agents [2–10]. In comparison to

*Corresponding author. Email: ccrl_2004@rediffmail.com, sns1963_1@rediffmail.com
† Present address: Department of Engineering Chemistry, ITM University, Gwalior, Madhya Pradesh, India.

ISSN 0095-8972 print/ISSN 1029-0389 online © 2012 Taylor & Francis
http://dx.doi.org/10.1080/00958972.2012.657630

the other anticancer agents ruthenium complexes show selective antimetastatic properties and lack of side effects.

Ruthenium(II) complexes of polypyridyl ligands have received much attention because of their rich electrochemical and photophysical properties [11–20]. Ruthenium polypyridyl complexes, such as $[Ru(bpy)_3]^{2+}$ (bpy = 2,2′-bipyridine), have potential applications in various fields, including the conversion of solar energy, sensing and signaling, therapeutic agents, and information storage [21]. The dinuclear ruthenium(II) polypyridyl system works as a multifunctional biological imaging agent staining the DNA of eukaryotic and prokaryotic cells [22]. Ruthenium(II) polypyridyl complexes are probes for DNA and hence potential therapeutic agents [23, 24].

Ruthenium complexes are much studied for their antibacterial and antifungal activities. Coordinating ruthenium to bioactive organic molecules often results in increased *in vitro* activity. A good example is ruthenium derivative of thiosemicarbazone; this exhibits a 70% increase in antibacterial activity against Gram-negative bacteria [25–27]. Ruthenium compounds are very well-suited for medicinal use because of their rate of ligand exchange, range of accessible oxidation states, and ability to mimic iron in binding to certain biological molecules.

We have selected 1,10-phenanthroline and 2,2′-bipyridine to develop new precursor molecules and 1,4-bis(salicylidene)phenylenediamine as a bidentate potential spacer since Schiff-base complexes derived from salicylaldehyde have shown promising results as antibacterial agents [28]. Here we explore the reaction of this spacer with ruthenium precursors which form dinuclear complexes with the possibility of better reactivity and enhanced pharmacological activity.

2. Experimental

$RuCl_3 \cdot 3H_2O$ (E. Merck), 1,4-phenylenediamine (CDH), salicylaldehyde (E. Merck), 1,10-phenanthroline (E. Merck), 2,2′-bipyridine, tetramethylene sulfoxide (Lancaster, UK), and Mueller Hinton Agar media (Himedia) were used as received. Analytical reagent dimethyl sulfoxide and routine solvents were used without purification.

Electronic absorption spectra were recorded with a Systronics 2201 UV-Vis double beam spectrophotometer equipped with a PC. Conductivity measurements were carried out at 25°C on an EI-181 digital conductivity bridge with a dipping type cell. FT-IR spectra were recorded in KBr pellets on a Shimadzu-8400 PC FT-IR spectrophotometer; $^{13}C\{^1H\}$-NMR, ^1H-NMR, and $\{^{13}C–^1H\}$2D-NMR (HETCOR) were recorded in D_2O/acetone on a DRX-300 MHz Bruker. Cobalt mercury tetrathiocyanate was used as standard. Diamagnetic correction was done using Pascal's constant. Elemental analyses (C, H, and N) were performed on an Elementra Vario EL III, Elemental Analyzer. Fast atom bombardment-mass spectra (FAB-MS) were recorded on a (JMS SX-102) Jeol Mass spectrometer using NBA as matrix.

2.1. *Synthesis of 1,4-bis(salicylidene)phenylenediamine, (SALPHEN)*

1,4-Phenylenediamine (0.1000 g; 1 mmol) was dissolved in 15 mL ethanol. To this solution salicylaldehyde (0.1880 mL; 2 mmol) was added and the reaction mixture was kept stirring for 1 h in an inert atmosphere (figure 1). Bright orange complex was

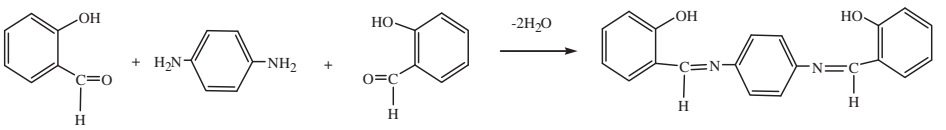

Figure 1. Reaction scheme for synthesis of ligand.

recovered on evaporation under reduced pressure. Yield: 0.23 g (79%); m.p. = 211°C; Found: C, 75.82; H, 5.59; N, 8.72. $C_{20}H_{16}N_2O_2$ ($M_\tau = 316.35$); Calcd: C, 75.93; H, 5.67; N, 8.85. Selected infrared absorption (KBr, cm^{-1}): ν(–CH=N), 1610(s); ν(Ar–OH), 3400(s); ^{1}H-NMR (300 MHz; acetone): δ9.1 (s, 2H, –CH=N), δ7.0 – 7.7 (m, 12H, Ar–H); δ11.0 (s, Ar–OH); $^{13}C\{^1H\}$-NMR (300 MHz; δ, acetone): δ164 (–CH=N), δ115–135 (Ar–C), δ160 (Ar–OH); FAB-MS $m/z = 316$.

2.2. *Synthesis of complexes*

The synthesis of each complex involves three steps.

2.2.1. Preparation of starting complexes. The four starting complexes were prepared by reported methods [29–31]. These complexes are [*cis*,*fac*-$RuCl_2$(DMSO-S)$_3$(DMSO-O)], [*trans*-$RuCl_2(DMSO)_4$], [*cis*-$RuCl_2(TMSO)_4$], and [*trans*-$RuCl_2(TMSO)_4$] which were recrystallized in suitable solvent mixture.

2.2.2. Preparation of precursor complexes. Recrystallized starting complex was dissolved in a small volume (~5 mL) of DMSO/TMSO. Into the above solution, 1,10-phenanthroline/2,2′-bipyridine dissolved in ~10 mL acetone was added in 1 : 1 molar ratio. The above reaction mixture was refluxed for 1–2 h and the color of the solution changed to red orange. This solution on vacuum evaporation yielded red orange solid which was recrystallized with 1 : 1 (v/v) mixture of diethylether : acetone. Totally eight precursors namely [*cis*-$RuCl_2(DMSO)_2$(phen)]; [*trans*-$RuCl_2(DMSO)_2$(phen)]; [*cis*-$RuCl_2(DMSO)_2$(bpy)]; [*trans*-$RuCl_2(DMSO)_2$bpy)]; [*cis*-$RuCl_2(TMSO)_2$(phen)]; [*trans*-$RuCl_2(TMSO)_2$(phen)]; [*cis*-$RuCl_2(TMSO)_2$(bpy)]; [*trans*-$RuCl_2(TMSO)_2$bpy] were synthesized.

2.2.3. Synthesis of dinuclear complexes. The recrystallized precursor (1 mmol) was dissolved in minimum quantity of DMSO/TMSO. The spacer 1,4-bis(salicylidene)phenylenediamine (1 mmol) dissolved in 10 mL of acetone was added to the above reaction mixture and kept under reflux for 1–8 h in an inert atmosphere. Color of the reaction mixture changed. The above solution was decanted and evaporated under vacuum resulting in microcrystals, which were washed several times with acetone and recrystallized from diethylether : acetone, 1 : 1 (v/v) mixture. In total eight complexes were synthesized; data are given below.

Complex 1, [{*cis*-$RuCl_2$(DMSO)(phen)}$_2$(μ-SALPHEN)] · DMSO
Yield: 0.10 g (87.71%); m.p. = 168°C; Found: C, 48.96; H, 3.75; N, 7.13; S, 5.43; Calcd: C, 48.98; H, 3.76; N, 7.14; S, 5.44. Δm at 25°C ($\Omega^{-1}\,cm^2\,mol^{-1}$): 54 in H_2O. Selected infrared absorption (KBr, cm^{-1}): ν(Ar–OH), 3410(b); ν(–CH=N), 1598(s); ν(so), 1099(s); ν(Ru–S), 456(s); ν(Ru–Cl), 321(sh); 335(s); ν(Ru–N), 272(s). Electronic

spectra (H_2O) λ_{max} (nm) (ε in $mol^{-1}\,cm^{-1}$): 714(94); 621(172); 577(207); 513(238); 472(508); 428(675); 378(792); ^{1}H-NMR (300 MHz; δ, D_2O): δ 9.95 (2H, –CH=N); δ 9.80–9.90, δ 10.00–10.80 (m, 16H, pyridyl-H); δ 7.68–7.12 (t, 12H, Ar–H); δ 3.90 (12H, CH_3); $^{13}C\{^1H\}$-NMR (300 MHz; δ, D_2O): δ 152.1 (–CH=N); δ 134.1–139.8 (pyridyl-C); δ 121.0–125.0 (Ar–C); δ 51.5 (S–C). FAB-MS m/z: $[RuCl]^+ = 136$, $[C_{14},H_{14}ClN_2OSRu^{101}]^+ = 394$, $[C_{14},H_{14}ClN_2OSRu^{102}]^+ = 395$, $[C_{20}H_{15}Cl_4N_2ORu^{101}]^+ = 641$, $[C_{20}H_{15}Cl_4N_2ORu^{102}]^+ = 642$, $[C_{34}H_{30}Cl_3N_4O_3SRu_2]^+ = 885$, $[C_{50}H_{50}N_6S_3O_5Cl_4Ru_2^{101}]^+ = 1253$, $[C_{50}H_{50}N_6S_3O_5Cl_3^{37}ClRu_2^{102}]^+ = 1255$; ($M_\tau = 1255$).

Complex 2, [{*trans*-$RuCl_2$(DMSO)(phen)}$_2$(μ-SALPHEN)] · DMSO

Yield: 0.09 g (78.9%); m.p. = 178°C; Found: C, 48.96; H, 3.75; N, 7.13; S, 5.43; Calcd: C, 48.98; H, 3.76; N, 7.14; S, 5.44. Δm at 25°C ($\Omega^{-1}\,cm^2\,mol^{-1}$): 42 in H_2O. Selected infrared absorption (KBr, cm^{-1}): ν(Ar–OH), 3415(b); ν(–CH=N), 1595(s); ν(so), 1082(s); ν(Ru–S), 440(s); ν(Ru–Cl), 328(sh); 335(s); ν(Ru–N), 276(s). Electronic spectra (H_2O) λ_{max} (nm) (ε in $mol^{-1}\,cm^{-1}$): 604(109); 542(192); 521(205); 496(312); 474(596); 452(602); 431(679); 412(715); 403(782); 392(849); ^{1}H-NMR (300 MHz; δ, D_2O): δ 9.85 (2H, –CH=N); δ 8.00–9.00, δ 9.90–10.50 (m, 16H, pyridyl-H); δ 7.30–7.70 (t, 12H, Ar–H); δ 3.60 (12H, CH_3). $^{13}C\{^1H\}$-NMR (300 MHz; δ, D_2O): δ 152.0 (–CH=N); δ 135.0–140.50 (pyridyl-C); δ 124.3–126.20 (Ar–C); δ 49.0 (S–C); FAB-MS m/z: $[RuCl]^+ = 136$, $[C_{12}H_8ClN_2Ru]^+ = 1316$, $[C_{14}H_{14}ClN_2OSRu^{101}]^+ = 394$, $[C_{14}, H_{14}ClN_2OSRu^{102}]^+ = 395$, $[C_{20}H_{15}Cl_4N_2ORu^{101}]^+ = 641$, $[C_{20}H_{15}Cl_4N_2ORu^{102}]^+ = 642$, $[C_{34}H_{30}Cl_3N_4O_3SRu_2]^+ = 885$, $[C_{50}H_{50}N_6S_3O_5Cl_4Ru_2^{101}]^+ = 1253$, $[C_{50}H_{50}N_6S_3O_5Cl_3ClRu_2^{102}]^+ = 1255$; ($M_\tau = 1255$).

Complex 3, [{*cis*-$RuCl_2$(DMSO)(bpy)}$_2$(μ-SALPHEN)] · DMSO

Yield: 0.03 g (51.72%); m.p. = 169°C; Found: C, 46.76; H, 3.91; N, 7.43; S, 5.67; Calcd: C, 46.81; H, 3.92; N, 7.44; S, 5.68. Δm at 25°C ($\Omega^{-1}\,cm^2\,mol^{-1}$): 49 in H_2O. Selected infrared absorption (KBr, cm^{-1}): ν(Ar–OH), 3412(b); ν(–CH=N), 1587(s); ν(so), 1084(s); ν(Ru–S), 459(s); ν(Ru–Cl), 328(sh); 335(s); ν(Ru–N), 275(s). Electronic spectra (H_2O) λ_{max} (nm) (ε in $mol^{-1}\,cm^{-1}$): 647(91); 523(264); 462(461); 445(512); 412(615); 374(781); ^{1}H-NMR (300 MHz; δ, D_2O): δ 9.92 (2H, –CH=N); δ 9.76–9.90, δ 10.01–10.60 (m, 2H, pyridyl-H); δ 7.12–7.60 (t, 12H, Ar–H); δ 3.95 (12H, CH_3); $^{13}C\{^1H\}$-NMR (300 MHz; δ, D_2O): δ 151.50 (–CH=N); δ 50.2 (S–C); δ 134.2–141.2 (pyridyl-C); δ 125.0–126.1 (Ar–C). FAB-MS m/z: $[RuCl]^+ = 136$, $[C_{10}H_8ClN_2Ru]^+ = 293$, $[C_{12}H_{14}ClN_2OSRu]^+ = 371$, $[C_{32}H_{30}ClN_4O_3SRu] = 687$, $[C_{44}H_{44}Cl_3N_6O_4S_2Ru_2^{101}]^+ = 1093$, $[C_{44}H_{44}Cl_3N_6O_4S_2Ru_2^{102}]^+ = 1095$, $[C_{44}H_{45}N_6S_2O_4Cl_4Ru_2]^+ = 1129$, $[C_{46}H_{50}Cl_4N_6O_5S_3Ru_2 + H^+] = 1207$; ($M_\tau = 1206$).

Complex 4, [{*trans*-$RuCl_2$(DMSO)(bpy)}$_2$(μ-SALPHEN)] · DMSO

Yield: 0.031 g (46.75%); m.p. = 158°C; Found: C, 46.76; H, 3.91; N, 7.43; S, 5.67; Calcd: C, 46.81; H, 3.92; N, 7.44; S, 5.68. Δm at 25°C ($\Omega^{-1}\,cm^2\,mol^{-1}$): 57 in H_2O. Selected infrared absorption (KBr, cm^{-1}): ν(Ar–OH), 3405(b); ν(–CH=N), 1588(s); ν(so), 1096(s); ν(Ru–S), 444(s); ν(Ru–Cl), 322(sh); 339(s); ν(Ru–N), 271(s). Electronic spectra (H_2O) λ_{max} (nm) (ε in $mol^{-1}\,cm^{-1}$): 635(97); 528(212); 479(381); 463(423); 415(602); 362(769); ^{1}H-NMR (300 MHz; δ, D_2O): δ 9.79 (2H, –CH=N); δ 7.72–9.60, δ 9.95–10.20 (m, 16H, pyridyl-H); δ 7.10–7.68 (t, 12H, Ar–H); δ 3.65 (12H, CH_3); $^{13}C\{^1H\}$-NMR (300 MHz; δ, D_2O): δ 152.6 (–CH=N); δ 135.5–141.8 (pyridyl-C); δ 128.5–130.0 (Ar–C); δ 43.3 (S–C); FAB-MS: $[RuCl]^+ = 136$, $[C_{10}H_8ClN_2Ru]^+ = 293$, $[C_{12}H_{14}ClN_2OSRu]^+ = 371$, $[C_{32}H_{30}ClN_4O_3SRu] = 687$, $[C_{44}H_{44}Cl_3N_6O_4S_2Ru_2^{101}]^+ = 1093$, $[C_{44}H_{44}Cl_3\ N_6O_4S_2Ru_2^{102}$

$C_{44}H_{44}Cl_3N_6O_4S_2Ru_2{}^{102}]^+ = 1095$, $[C_{44}H_{45}N_6S_2O_4Cl_4Ru_2]^+ = 1129$, $[C_{46}H_{50}Cl_4N_6O_5S_3Ru_2 + H^+] = 1207$; ($M_\tau = 1206$).

Complex 5, [{*cis*-RuCl$_2$(TMSO)(phen)}$_2$(μ-SALPHEN)] · TMSO

Yield: 0.10 g (90.74%); m.p. = 172°C; Found: C, 50.79; H, 3.91; N, 6.85; S, 5.20; Calcd: C, 50.81; H, 3.93; N, 6.83; S, 5.21. Δm at 25°C ($\Omega^{-1}\,cm^{-2}\,mol^{-1}$): 59 in H_2O. Selected infrared absorption (KBr, cm^{-1}): ν(Ar–OH), 3414(b); ν(–CH=N), 1571(s); ν(so), 1121(s); ν(Ru–S), 454(s); ν(Ru–Cl), 321(sh); 330(s); ν(Ru–N), 272(s). Electronic spectra (H_2O) λ_{max} (nm) (ε in $mol^{-1}\,cm^{-1}$): 761(85); 652(192); 621(201); 492(290); 479(394); 412(478); 403(517); 361(681); ^{1}H-NMR (300 MHz; δ, D_2O): δ 9.76–9.85, δ 10.10–10.60 (m, 16H, pyridyl-H); δ 9.91 (2H, –CH=N); δ 7.2–7.60 (t, 12H, Ar–H); δ 4.23 (8H, S–CH_2); δ 3.52 (8H, S–C–CH_2); ^{13}C{^{1}H}-NMR (300 MHz; δ, D_2O): δ 152.2 (–CH=N); δ 134.5–139.9 (pyridyl-C); δ 127.1–129.5 (Ar–C); δ 57.6 (S–C); δ 27.4 (S–C–C); FAB-MS: $[RuCl]^+ = 136$, $[C_{12}H_8ClN_2Ru]^+ = 317$; $[C_{16}H_{16}ClN_2OSRu]^+ = 421$, $[C_{36}H_{32}ClN_4O_3SRu]^+ = 737$, $[C_{52}H_{48}Cl_3N_6O_4S_2Ru_2]^+ = 1195$, $[C_{52}H_{48}Cl_4N_6O_4S_2Ru_2 + H]^+ = 1230$, $[C_{56}H_{56}Cl_4N_6O_5S_3Ru_2 + H]^+ = 1335$; ($M_\tau = 1334$).

Complex 6, [{*trans*-RuCl$_2$(TMSO)(phen)}$_2$(μ-SALPHEN)] · TMSO

Yield: 0.029 g (66.44%); m.p. = 165°C; Found: C, 50.79; H, 3.91; N, 6.85; S, 5.20; Calcd: C, 50.81; H, 3.93; N, 6.83; S, 5.21. Δm at 25°C ($\Omega^{-1}\,cm^2\,mol^{-1}$): 56 in H_2O. Selected infrared absorption (KBr, cm^{-1}): ν(Ar–OH), 3410(b); ν(–CH=N), 1572(s); ν(so), 1127(s); ν(Ru–S), 454(s); ν(Ru–Cl), 337(s); 333(sh); ν(Ru–N), 274(s). Electronic spectra (H_2O): λ_{max} (nm) (ε in $mol^{-1}\,cm^{-1}$): 689(81); 578(128); 532(195); 478(392); 445(421); 430(492); 409(517); 367(621). ^{1}H-NMR (300 MHz; δ, D_2O): δ 9.72 (2H, –CH=N); δ 7.71–9.50, δ 10.04–10.30 (m, 16H, pyridyl-H); δ 7.2–7.60 (t, 12H, Ar–H); δ 3.96 (8H, S–CH_2); δ 3.43 (8H, S–C–CH_2). ^{13}C{^{1}H}-NMR (300 MHz; δ, D_2O): δ 152.40 (–CH=N); δ 135.3–142.3 (pyridyl-C); δ 126.4–128.4 (Ar–C); δ 52.3 (S–C); δ 26.3 (S–C–C). FAB-MS: $[RuCl]^+ = 136$, $[C_{12}H_8ClN_2Ru]^+ = 317$, $[C_{16}H_{16}ClN_2OSRu]^+ = 421$, $[C_{36}H_{32}ClN_4O_3SRu]^+ = 737$, $[C_{52}H_{48}Cl_3N_6O_4S_2Ru_2]^+ = 1195$, $[C_{52}H_{48}Cl_4N_6O_4S_2Ru_2 + H]^+ = 1230$, $[C_{56}H_{56}Cl_4N_6O_5S_3Ru_2 + H]^+ = 1335$; ($M_\tau = 1334$).

Complex 7, [{*cis*-RuCl$_2$(TMSO)(bpy)}$_2$(μ-SALPHEN)] · TMSO

Yield: 0.08 g (72.99%); m.p. = 173°C; Found: C, 48.46; H, 4.09; N, 7.12; S, 5.41; Calcd: C, 48.81; H, 4.09; N, 7.11; S, 5.43. Δm at 25°C ($\Omega^{-1}\,cm^2\,mol^{-1}$): 49 in H_2O. Selected infrared absorption (KBr, cm^{-1}): ν(Ar–OH), 3412(b); ν(–CH=N), 1573(s); ν(so), 1131(s); ν(Ru–S), 461(s); ν(Ru–Cl), 334(s); 339(sh); ν(Ru–N), 271(s). Electronic spectra (H_2O): λ_{max} (nm) (ε in $mol^{-1}\,cm^{-1}$): 694(71); 571(185); 492(216); 445(298); 421(398); 405(472); 362(621). ^{1}H-NMR (300 MHz; δ, D_2O): δ 9.77–9.80, δ 10.05–10.34 (m, 16H, pyridyl-H); δ 9.89 (2H, –CH=N); δ 7.1–7.63 (t, 12H, Ar–H); δ 4.28 (8H, S–CH_2); δ 3.46 (8H, S–C–CH_2). ^{13}C{^{1}H}-NMR (300 MHz; δ, D_2O): δ 151.5 (–CH=N); δ 134.2–138.0 (pyridyl-C); δ 127.0–130.0 (Ar–C); δ 57.4 (S–C); δ 25.7 (S–C–C); FAB-MS: $[RuCl]^+ = 136$; $[C_{10}H_8ClN_2Ru]^+ = 293$; $[C_{14}H_{16}ClN_2OSRu]^+ = 397$; $[C_{34}H_{32}ClN_4O_3SRu]^+ = 713$; $[C_{48}H_{48}Cl_3N_6O_4S_2Ru_2]^+ = 1147$; $[C_{48}H_{48}Cl_4N_6O_4S_2Ru_2 + H]^+ = 1182$; $[C_{52}H_{56}Cl_4N_6O_5S_3Ru_2 + H]^+ = 1287$; ($M_\tau = 1286$).

Complex 8, [{*trans*-RuCl$_2$(TMSO)(bpy)}$_2$(μ-SALPHEN)] · TMSO

Yield: 0.021 g (67.32%); m.p. = 161°C; Found: C, 48.46; H, 4.09; N, 7.12; S, 5.41; Calcd: C, 48.81; H, 4.09; N, 7.11; S, 5.43. Δm at 25°C ($\Omega^{-1}\,cm^2\,mol^{-1}$): 58 in H_2O. Selected infrared absorption (KBr, cm^{-1}): ν(Ar–OH), 3408(b); ν(–CH=N), 1587(s); ν(so), 1127(s); ν(Ru–S), 454(s); ν(Ru–Cl), 337(s); 333(sh); ν(Ru–N), 274(s). Electronic

spectra (H_2O) λ_{max} (nm) (ε in $mol^{-1}\,cm^{-1}$): 681(93); 523(206); 493(298); 475(331); 435(417); 401(519); 355(612). ^{1}H-NMR (300 MHz; δ, D_2O): δ 9.73 (2H, –CH=N); δ 7.71–9.65, δ 9.90–10.10 (m, 16H, pyridyl-H); δ 7.11–7.60 (t, 12H, Ar–H); δ 3.92 (8H, S–CH_2); δ 3.42 (8H, S–C–CH_2); $^{13}C\{^1H\}$-NMR (300 MHz; δ, D_2O): δ 152.8 (–CH=N); δ 135.1–141.5 (pyridyl-C); δ 126.0–129.1 (Ar–C); δ 51.1 (S–C); δ 26.9 (S–C–C). FAB-MS m/z $[RuCl]^+ = 136$; $[C_{10}H_8ClN_2Ru]^+ = 293$; $[C_{14}H_{16}ClN_2OSRu]^+ = 397$; $[C_{34}H_{32}ClN_4O_3SRu]^+ = 713$; $[C_{48}H_{48}Cl_3N_6O_4S_2Ru_2]^+ = 1147$; $[C_{48}H_{48}Cl_4N_6O_4S_2Ru_2 + H]^+ = 1182$; $[C_{52}H_{56}Cl_4N_6O_5S_3Ru_2 + H]^+ = 1287$; ($M_\tau = 1286$).

2.3. *Antibacterial activity*

Complexes **1**–**8**, their precursors **1a**–**8a**, and the ligand were screened for antibacterial activity against Gram-negative bacteria *Escherichia coli* MTCC 1304 at different concentrations. Mueller-Hinton agar (MHA) plates were prepared and 50 µL suspensions of *E. coli* containing approximately 10^5 CFU (colony forming unit) were applied to the plate by spread plate technique [32]. Wells were made on the plates and filled with 50 µL of sample solution of 0.02% and 0.03% concentrations prepared in distilled water. Chloramphenicol (0.02% solution) was used for comparison. These plates were incubated at 37 ± 1°C for 24–48 h in refrigerated incubator shakers. The results in the form of zone inhibition were measured in millimeters.

3. Results and discussion

3.1. *Characterization of ligand*

The C, H, and N analytical data for the synthesized ligand are in agreement with the proposed empirical formula. FAB-MS of ligand shows pseudomolecular ion peak at $m/z = 316$, confirming the molecular weight of the ligand. In FT-IR spectra of the ligand a broad absorption was observed at 3400 cm^{-1} for aromatic hydroxyl group. A sharp peak at 1610 cm^{-1} was assigned to the presence of azomethine (–CH=N). In the ^{1}H-NMR spectrum a signal at δ 9.1 ppm was attributed for (–CH=N) group. Multiplets observed from δ 7.0–7.7 ppm were assigned for aromatic proton (Ar–H). The signal at δ 11.0 ppm was assigned for aromatic hydroxyl group (–OH). The $^{13}C\{^1H\}$-NMR exhibited a signal at δ 164 ppm, assigned for –CH=N carbon. The signals in the range δ 119–168 ppm were attributed for (Ar–C) carbon.

The ligand was also characterized on the basis of $\{^{13}C–^1H\}$2D-NMR (HETCOR). In 2D-NMR spectra of ligand the signal at δ 160 ppm for C-1 is connected to H-1 of –OH. The aromatic carbon C-2 at δ 124 ppm is connected to H-2 at δ 7.6 ppm, similarly C-3 at δ 7.51 ppm is connected to H-3 at δ 7.45 ppm, C-4 at δ 135 ppm is connected to H-4 at δ 7.51 ppm, and C-5 at δ 134 ppm is connected to H-5 at δ 7.7 ppm. Carbon at C6 appears at δ 115 ppm. The azomethine carbon (–HC=N) C-7 at δ 164 ppm was found to be connected to H-7 at δ 9.1 ppm [33, 34]. The four equivalent carbons of the aromatic amine ring C-9 at δ 120 ppm were connected to H-9 at δ 7.08 ppm and the carbon C-8 was found at δ 118 ppm.

Thus on the basis of FT-IR, $\{^{13}C–^1H\}$2D-NMR, elemental analysis, and FAB-mass studies the reaction scheme and most probable structure of the ligand are suggested in figure 2.

3.2. *Characterization of ruthenium complexes*

Empirical formulae of **1–8** were in conformity with the elemental analysis. Molecular weights of all the complexes were determined by FAB-MS. A number of peaks were observed in mass spectra. Some important peaks, which were spotted in the FAB-mass of all the complexes, are $[RuCl]^+$, $[RuCl(bpy)]^+$, $[RuCl(bpy)(so)]^+$, $[RuCl(bpy)(so)(SALPHEN)]^+$, $[RuCl_2(bpy)(so)(\mu\text{-SALPHEN})RuCl(bpy)(so)]^+$, $[RuCl_2(bpy)(so)(\mu\text{-SALPHEN})RuCl_2(bpy)(so)+H]^+$, and $[\{RuCl_2(bpy)(so)(\mu\text{-SALPHEN})RuCl_2(bpy)(so)\}.so+H^+]$. Ruthenium has six isotopes with significant natural abundance (>15%) from 96 to 104, therefore, in some complexes isotopic mass peaks assigned for Ru^{101} and Ru^{102} were also observed. Since in FAB-mass metal complexes never give parent ion peak as molecular ion, the ion of highest molecular mass observed in the spectrum is the complex ion [35, 36]. The molecular conductance values for a very dilute solution ($\sim$0.001 mol L^{-1}) are 42–59 Ω^{-1} cm^2 mol^{-1} for all the complexes, in the range suggested for 1 : 1 electrolytes [37], explained on the basis that in solution one chloride is replaced by solvent. Some important data are given in table 1.

3.2.1. Electronic spectral study. All complexes were diamagnetic (low spin d^6) as expected for ruthenium(II) complexes. Since ruthenium polypyridyl complexes are identified as a particularly efficient photosensitizer because of their broad range of visible light absorption, here all complexes displayed six to ten bands in electronic spectra. Two/three less intense absorptions observed in visible region between 662–651 nm and 564–557 nm were d–d transition corresponding to $^1A_{1g} \rightarrow {}^1T_{1g}$ and $^1A_{1g} \rightarrow {}^1T_{2g}$, respectively. Two bands at 410 nm and 425 nm were designated to

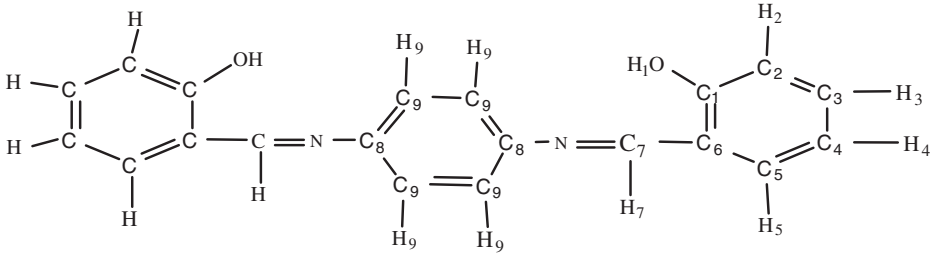

Figure 2. Structure of ligand.

Table 1. Color, yield, and melting points.

Complexes	Color	Yield (%)	m.p.
1,4-bis(salicylidene)phenylenediamine (μ-SALPHEN)	Bright orange	0.230 g (79)	211
[{*cis*-$RuCl_2$(DMSO)phen}$_2$(μ-SALPHEN)] · DMSO	Dark green	0.100 g (87.71)	168
[{*trans*-$RuCl_2$(DMSO)phen}$_2$(μ-SALPHEN)] · DMSO	Dark green	0.090 g (78.9)	178
[*cis*-$RuCl_2$(DMSO)bypy}$_2$(μ-SALPHEN)] · DMSO	Dark brown	0.030 g (51.72)	169
[{*trans*-$RuCl_2$(DMSO)bypy}$_2$(μ-SALPHEN)] · DMSO	Brown	0.031 g (46.75)	158
[{*cis*-$RuCl_2$(TMSO)phen}$_2$(μ-SALPHEN)] · TMSO	Dark brown	0.100 g (90.74)	172
[{*trans*-$RuCl_2$(TMSO)phen}$_2$(μ-SALPHEN)] · TMSO	Brown	0.029 g (66.44)	165
[{*cis*-$RuCl_2$(TMSO)$_2$bypy}$_2$(μ-SALPHEN)] · TMSO	Brown	0.080 g (72.99)	173
[{*trans*-$RuCl_2$(TMSO)bypy}$_2$(μ-SALPHEN)] · TMSO	Brown	0.021 g (67.32)	161

intraligand transitions $\pi - \pi^*$ and $n - \pi^*$ non-bonding electrons present on nitrogen of the azomethine in the Schiff-base complexes, respectively. Five bands with high extinction coefficient between 435 and 492 nm were assigned to metal-to-ligand charge transfer (MLCT) transition. Three MLCT transitions between 435 and 465 nm are due to two different acceptor levels in 2,2′-bipyridine\1,10-phenanthroline and two bands between 470 and 492 nm are due to transfer of lone pair from azomethine nitrogen to the metal. More than double enhancement of the absorbance in dinuclear complexes as compared to mononuclear precursor complexes could be considered from the presence of two ruthenium(II) centers [38–41].

3.2.2. Infrared spectral study. The broad absorption band for phenolic ν(Ar–OH) was observed at 3400 cm^{-1} in the free ligand. In the complexes the band was observed almost at the same place, indicating non-involvement of –OH in coordination. Absorption at 1610 cm^{-1} was assigned for ν(–CH=N) in the ligand [34, 35]. In all the complexes a shift was observed to lower energy by 35–40 cm^{-1}. Peak intensity was decreased from the free ligand spectra, indicating that the two metal centers were symmetrically coordinated to nitrogen atoms of ligand [42].

In all the complexes one peak at 1082–1131 cm^{-1} was assigned for ν(so). Another peak at 1044–1062 cm^{-1} was assigned for DMSO/TMSO present outside the coordination sphere [43–45]. A weak band at 460 cm^{-1} was assigned for ν(Ru–S).

3.2.3. ^{1}H-NMR spectra. In ^{1}H-NMR spectra (table 2) of all the Ru(II) complexes signals for pyridine protons were observed at δ 7.71–9.0 ppm and δ 9.9–10.80 ppm. In the ^{1}H-NMR spectra of **1**, **2**, **3**, and **4** two signals were observed for methyl proton of DMSO. In **1** and **3**, one signal centered at δ 3.90 ppm for 12 protons was attributed to methyl of DMSO anti to Cl^- at both ruthenium centers. Both complexes exhibit signal at δ 2.40 ppm for six protons for methyl of free DMSO [46]. In **2** and **4** signal at δ 3.60 ppm for 12 protons was attributed to methyl group of DMSO *trans* to pyridyl-*N*. The singlet observed at δ 2.50 ppm for six protons was assigned to DMSO outside the coordination sphere.

In the TMSO analogs, **5**, **6**, **7**, and **8**, three signals were observed for methylene. In **5** and **7**, a multiplet centered at δ 4.28 ppm for eight protons was attributed to S–CH_2 of TMSO situated anti to Cl^- at both ruthenium centers [47]. The multiplet centered at δ 3.70 ppm for four protons was assigned to S–CH_2 of free TMSO; multiplet centered at δ 3.50 ppm was assigned for all 12 protons of S–C–CH_2 of TMSO. In **6** and **8**, a multiplet centered at δ 3.90 ppm for eight protons was assigned for S–CH_2 of TMSO *trans* to pyridyl-*N* [48]. A multiplet centered at δ 3.40 ppm was attributed for 12 protons of S–C–CH_2 of TMSO and the multiplet centered at δ 3.70 for four protons was attributed for S–CH_2 of free TMSO.

A broad signal observed at δ 9.90 ppm for two protons was assigned to azomethine (–CH=N). This signal is at higher δ value than that of ligand, which confirms the involvement of azomethine-*N* in coordination.

In the ^{1}H-NMR spectra of TMSO complexes multiplets were observed at δ 3.92 ppm and δ 3.96 ppm, for eight protons, assigned for S–CH_2 protons of TMSO *trans* to Cl and at δ 4.23 ppm and δ 4.28 ppm for S–CH_2 protons of TMSO *cis* to Cl. The spectra of TMSO complexes showed singlets at δ 3.96 ppm and δ 4.23 ppm assigned for S–C–CH_2 of TMSO *trans* to Cl and *cis* to Cl, respectively. In ^{1}H-NMR spectra of all the Ru(II)

Table 2. ^{1}H-NMR data (δ values in ppm) of complex.

Complexes	δ(Pyridyl-H)	δ(Ar–H)	δ(HC=N)	δ(CH_3)	δ(S–CH_2)	δ(S–C–CH_2)
μ-SALPHEN (Ligand before coordination)	–	H_2-7.6(s, 2H) H_3-7.45(d, 2H) H_4-7.51(d, 2H) H_5-7.7(s, 2H) H_9-7.08	H_7-9.1	–	–	–
[{*cis*-$RuCl_2$(DMSO)phen}$_2$(μ-SALPHEN)] · DMSO	9.80–9.90, 10.00–10.80 (m, 16H)	7.12–7.68 (m, 12H)	9.95 (s, 2H)	3.9(12H) 2.45(6H)	–	–
[{*trans*-$RuCl_2$(DMSO)phen}$_2$(μ-SALPHEN)] · DMSO	8.00–9.00, 9.90–10.50 (m, 16H)	7.30–7.7 (m, 12H)	9.85 (s, 2H)	3.6(12H) 2.5(6H)	–	–
[*cis*-$RuCl_2$(DMSO)bpy}$_2$(μ-SALPHEN)] · DMSO	9.76–9.90, 10.01–10.60 (m, 16H)	7.12–7.60 (m, 12H)	9.92 (s, 2H)	3.95(12H) 2.47(6H)	–	–
[{*trans*-$RuCl_2$(DMSO)bpy}$_2$(μ-SALPHEN)] · DMSO	7.72–9.60, 9.95–10.20 (m, 16H)	7.10–7.68 (m, 12H)	9.79 (s, 2H)	3.65(12H) 2.49(6H)	–	–
[{*cis*-$RuCl_2$(TMSO)phen}$_2$(μ-SALPHEN)] · TMSO	9.76–9.85, 10.10–10.60 (m, 16H)	7.20–7.60 (m, 12H)	9.91 (s, 2H)	–	4.23(8H) 3.70(4H)	3.52(12H)
[{*trans*-$RuCl_2$(TMSO)phen}$_2$(μ-SALPHEN)] · TMSO	7.71–9.50, 10.04–10.30 (m, 16H)	7.2–7.60 (m, 12H)	9.72 (s, 2H)	–	3.96(8H) 3.63(4H)	3.43(12H)
[{*cis*-$RuCl_2$($TMSO)_2$bpy}$_2$(μ-SALPHEN)] · TMSO	9.77–9.80, 10.05–10.34 (m, 16H)	7.1–7.63 (m, 12H)	9.89 (s, 2H)	–	4.28(8H) 3.71(4H)	3.46(12H)
[{*trans*-$RuCl_2$(TMSO)bpy}$_2$(μ-SALPHEN)] · TMSO	7.71–9.65, 9.90–10.10 (m, 16H)	7.11–7.60 (t, 12H, Ar–H)	9.73 (s, 2H)	–	3.92(8H) 3.72(4H)	3.42(12H)

complexes sharp signals were observed at δ 2.40 ppm in DMSO and δ 3.70 ppm in TMSO analog, indicating the presence of uncoordinated DMSO/TMSO in all Ru(II) complexes.

3.2.4. $^{13}C\{^1H\}$-NMR spectra. Complexes were also studied on the basis of $^{13}C\{^1H\}$-NMR spectroscopy. Signals at δ 134.1–142.3 ppm were assigned for pyridine carbons [34, 35]. Similarly signals between δ 121.0–130.0 ppm were attributed to aromatic carbons. A signal at δ 164.0 ppm in the ligand that shifted to δ 152.0 ppm in the complexes was assigned for azomethine carbon.

In the DMSO complexes two signals were observed for S–C carbon of DMSO. The signal at δ 50.0 ppm was attributed to S–C carbon *trans* to Cl/bipyridine nitrogen and the signal at δ 35.0 ppm was assigned for S–C carbon of free DMSO. In TMSO analogs three signals were observed. In **5** and **7,** the signal at δ 57.0 ppm was assigned for S–C carbon of TMSO *trans* to Cl. However, **6** and **8** exhibit a signal at δ 52.0 ppm for S–C carbon of TMSO *trans* to bipyridine nitrogen [49–51]. In all TMSO analogs a signal at δ 50.0 ppm was attributed to S–C carbon of free TMSO. Also in all the complexes only one signal between δ 25.7–27.4 ppm was assigned to S–C–C carbon of TMSO.

3.2.5. $\{^{13}C–^1H\}$2D-NMR (HETCOR) spectrum. In $\{^{13}C–^1H\}$2D-NMR spectrum of **2** (Supplementary material) pyridyl carbons in the range δ 134.1–139.8 ppm were connected to pyridyl protons at δ 8.0–9.0 ppm as multiplets. The aromatic carbons of the spacer ligand were at δ 124.3–126 ppm and were connected to the aromatic protons in the range δ 7.30–7.70 ppm. The azomethine carbon (–CH=N) at δ 152 ppm is connected to the azomethine proton at δ 9.85 ppm [34, 35]. The peak at δ 49.0 ppm for the DMSO carbon was found connected to the DMSO methyl at δ 3.6 ppm; also in free or uncoordinated DMSO peak of carbon at δ 35.5 ppm was found connected to DMSO methyl proton at δ 2.5 ppm.

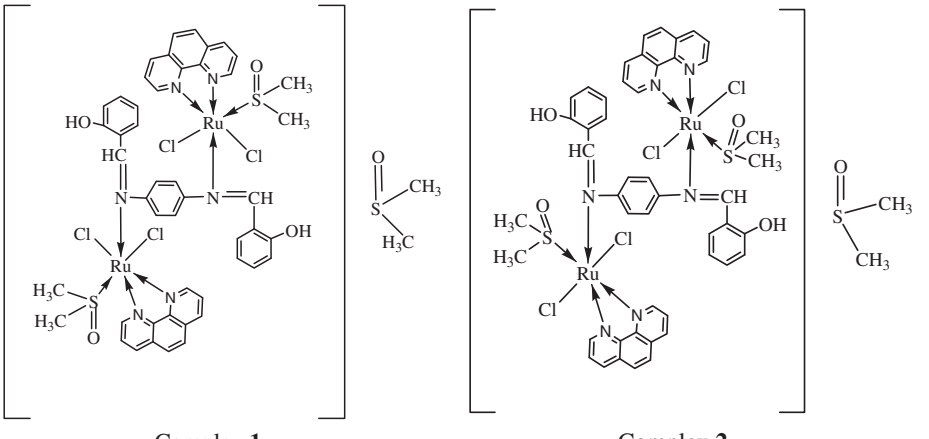

Complex **1** Complex **2**

Figure 3. Structure of complexes **1–8**.

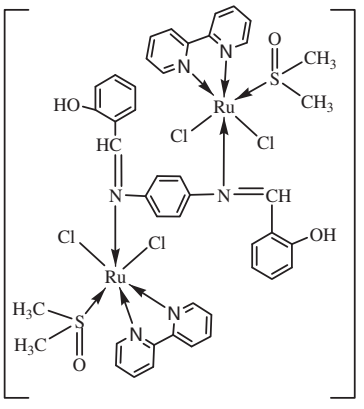

Complex **3**

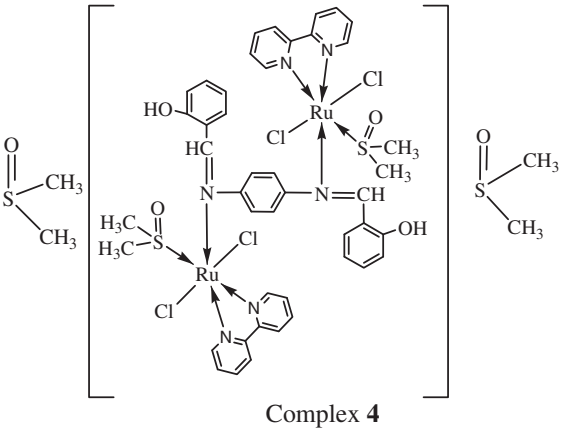

Complex **4**

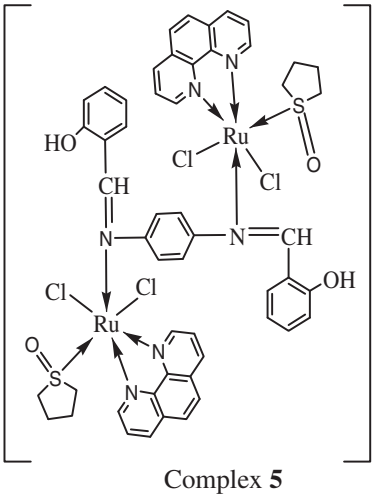

Complex **5**

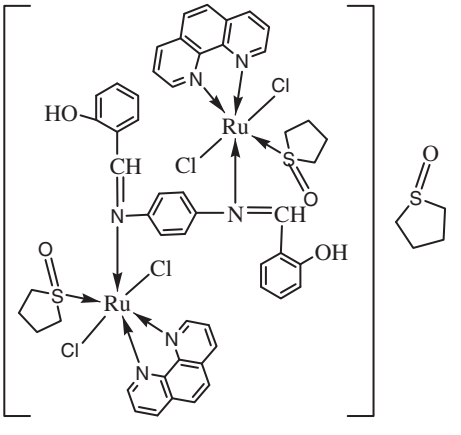

Complex **6**

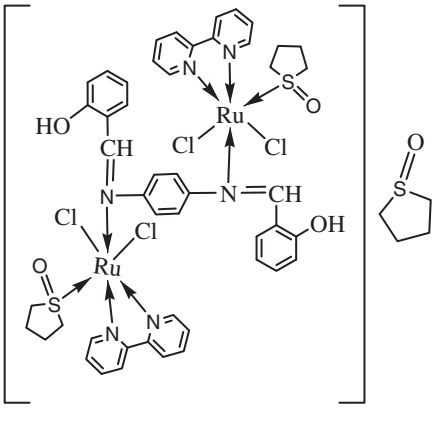

Complex **7**

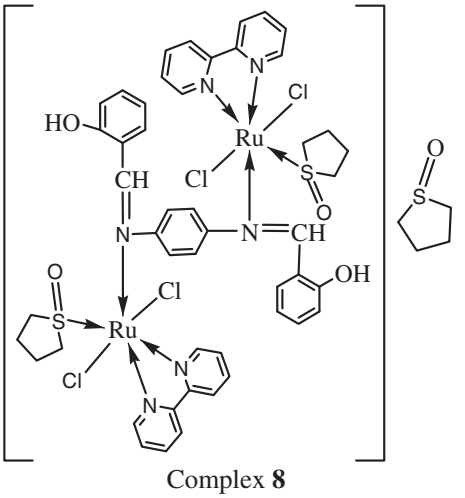

Complex **8**

Figure 3. Continued.

Table 3. Antibacterial screening against *E. coli*.

Complex/precursor	Diameter of inhibition zone (in mm) ± SEM
SALPHEN	9 ± 0.7
[{*cis*,*fac*-$RuCl_2$(DMSO)phen}$_2$(μ-SALPHEN)] · DMSO	18 ± 0.5
[*cis*,*fac*-$RuCl_2$(DMSO)$_2$phen]	9 ± 0.8
[{*trans*-$RuCl_2$(DMSO)phen}$_2$(μ-SALPHEN)] · DMSO	14 ± 1
[*trans*-$RuCl_2$(DMSO)$_2$phen]	8 ± 1.0
[{*cis*,*fac*-$RuCl_2$(DMSO)bpy}$_2$(μ-SALPHEN)] · DMSO	15 ± 0.5
[*cis*,*fac*-$RuCl_2$(DMSO)$_2$bpy]	8 ± 0.8
[{*trans*-$RuCl_2$(DMSO)bpy}$_2$(μ-SALPHEN)] · DMSO	19 ± 1.0
[*trans*-$RuCl_2$(DMSO)$_2$bpy]	9 ± 0.9
[{*cis*,*fac*-$RuCl_2$(TMSO)phen}$_2$(μ-SALPHEN)] · TMSO	15 ± 1
[*cis*,*fac*-$RuCl_2$(TMSO)$_2$phen]	7 ± 0.5
[{*trans*-$RuCl_2$(TMSO)phen}$_2$(μ-SALPHEN)] · TMSO	20 ± 1
[*trans*-$RuCl_2$(TMSO) $_2$phen]	8 ± 0.8
[{*cis*,*fac*-$RuCl_2$(TMSO)$_2$bpy}$_2$(μ-SALPHEN)] · TMSO	17 ± 1
[*cis*,*fac*-$RuCl_2$(TMSO)$_2$bpy]	6 ± 0.5
[{*trans*-$RuCl_2$(TMSO)bpy}$_2$(μ-SALPHEN)] · TMSO	19 ± 1
[*trans*-$RuCl_2$(TMSO) $_2$bpy]	9 ± 0.8
Chloramphenicol	40 ± 0.9

3.2.6. Biological activity. All ruthenium complexes show more activity against *E. coli* (table 3) than ligand and precursors, which are also bioactive. The results of antibacterial screening for 0.02% concentration are given in table 3, compared against Chloramphenicol. Complex **6** shows highest inhibition zone of 20 mm. These complexes exhibit the same range of antibacterial activity as deciphered earlier by dimeric Ru(II) 5-nitro-*o*-phenanthroline chlorosulfoxide complexes [52].

4. Conclusion

A dinucleating spacer 1,4-bis(salicylidene)phenylenediamine was synthesized by condensation of 1,4-phenylenediamine and salicylaldehyde in ethanol. Eight dinuclear Ru(II) complexes (figure 3) have been synthesized by reaction between one mole of spacer and two mole of ruthenium precursor. One DMSO was replaced from each precursor unit and Schiff base spacer ligand links the two precursor units to yield a dimer consisting of octahedral ruthenium at each center. The ruthenium dimeric complexes are more biologically active than monomeric precursors and Schiff base spacer ligand, against *E. coli*.

Acknowledgments

We are grateful to our Principal, Govt. Model Science College, Jabalpur and Head, Department of Chemistry, Govt. Model Science College, Jabalpur for providing laboratory facilities. Thanks are also due to SAIF, CDRI, Lucknow for C, H, and N analyses and {^{13}C–^{1}H}2D-NMR (HETCOR) spectra. We are indebted to Dr K.K. Verma, Retired Professor, Department of Chemistry, RDVV, Jabalpur and

to Dr K.K. Mishra, Retired Professor, Department of Chemistry, RDVV, Jabalpur for their help rendered in IR and UV spectra. SNS is grateful to UGC for the sanction of a Major Research Project.

References

[1] A. Mathieu, J. Gueniat, B. Therrien, G. Suss-Fink, A.K. Renfrew, P.J. Dyson. *J. Organomet. Chem.*, **694**, 855 (2009).
[2] I. Bartsos, S. Jedner, T. Gianferrara, E. Alessio. *Int. J. Chem.*, **61**, 692 (2007).
[3] E. Alessio. *Chem. Rev.*, **104**, 4203 (2004).
[4] E. Iengo, G. Mestroni, S. Geremia, M. Calligaris, E. Alessio. *J. Chem. Soc., Dalton Trans.*, 3371 (1999).
[5] A.J. Wright, C. Brodie, E. Glazer, N.W. Luedtke, L.E. Schwab, Y. Tor. *Chem. Commun.*, 1018 (2004).
[6] O.V. Gijte, D. Kirsch, A.A. Mesmaeker. *J. Chem. Soc., Dalton Trans.*, 951 (1999).
[7] A. Brodkorb, D. Krisch, A.A. Mesmaeker, T. Rutherford, F.R. Keene. *Eur. J. Inorg. Chem.*, 2151 (2001).
[8] R.S. Srivastava, F. Fronezek, L.M. Romero. *Inorg. Chim. Acta*, **357**, 2410 (2004).
[9] P.J. Dyson, G. Sava. *Dalton Trans.*, 1929 (2006).
[10] W. Nawrocka. *Boll. Chim. Farm.*, **135**, 18 (1996).
[11] D.A. Lutterman, A.A. Rachford, J.J. Rack, C. Tirro. *J. Phys. Chem. A*, **113**, 11002 (2009).
[12] V. Balzani, A. Juris, M. Venturi, S. Campagna, S. Serroni. *Chem. Rev.*, **96**, 759 (1996).
[13] M. Venturi, S. Serroni, A. Juris, S. Campagna, V. Balzani. *Top. Curr. Chem.*, **197**, 193 (1998).
[14] L. DeCola, P. Belser. *Coord. Chem. Rev.*, **177**, 301 (1998).
[15] V. Balzani, S. Campagna, G. Denti, A. Juris, S. Serroni, M. Venturi. *Acc. Chem. Res.*, **31**, 26 (1998).
[16] P. Belser, S. Bernhard, C. Blum, A. Beyerler, L. DeCola, V. Balzani. *Coord. Chem. Rev.*, **155**, 190 (1999).
[17] F. Barigelletti, L. Flamignu. *Chem. Soc. Rev.*, **29**, 1 (2000).
[18] A. Ei-Ghayoury, A. Harriman, A. Khatyr, R. Ziessel. *Angew. Chem., Int. Ed. Engl.*, **39**, 185 (2000).
[19] F. Schramm, R. Chandrasekar, T.A. Zevaco, M. Rudolph, H. Görls, W. Poppitz, M. Ruben. *Eur. J. Inorg. Chem.*, 53 (2009).
[20] O.X. Zhou, W.H. Lei, J.R. Chen, C. Li, Y.J. Hou, X.S. Wang, B.W. Zhang. *Chem. Eur. J.*, **16**, 3157 (2010).
[21] S.N. Shukla, P. Gaur, H. Kaur, M. Prasad. *J. Coord. Chem.*, **60**, 1047 (2007).
[22] M.R. Gill, L.J. Garcia, S.J. Foster, C. Smythe, G. Battaglia, J. Thomas. *Nature Chem.*, **1**, 662 (2009).
[23] M.C. Prabhakara, B.B. Basvaraju, H.S. Naik. *Bioinorg. Chem. Appl.*, 136 (2007).
[24] P.J. Dyson, G. Sava. *Dalton Trans.*, 1929 (2006).
[25] B. Centinkaya, I. Ozdemir, B. Binbasioglu, R. Durmaz, S. Gunal. *Arzneimittelforschung*, **49**, 538 (1999).
[26] I. Turel, J. Kljun, F. Perdih, E. Morozova, V. Bakulev, N. Kasyanenko, J.A.W. Byl, N. Osheroff. *Inorg. Chem.*, **49**, 10750 (2010).
[27] T.D. Thangadurai, S. Jeong, S. Yun, S. Kim, C. Kim, Y. Lee. *Microchem. J.*, **95**, 235 (2009).
[28] F.M. Morad, M.M.E. Lajaily, S.B. Gweirif. *J. Sci. Appl.*, **1**, 72 (2007).
[29] I.P. Evans, A. Spencer, G. Wilkinson. *J. Chem. Soc., Dalton Trans.*, 204 (1973).
[30] E. Alessio, G. Mestroni, G. Nardin, W.M. Attia, M. Calligaris, G. Sava, S. Zorzet. *Inorg. Chem.*, **27**, 4099 (1988).
[31] E. Alessio, B. Milani, G. Mestroni, P. Faleschini, W.M. Attia, M. Calligaris. *Inorg. Chim. Acta*, **177**, 255 (1990).
[32] M.J. Pelczar, E.C.S. Chan, N.R. Kreig. *Text Book of Microbiology*, Vol. 138, 5th Edn, Vol. 138, McGraw Hill, New Delhi, India (2000).
[33] R.M. Silverstein, G.C. Bassler, T.C. Morrill. *Spectrometric Identification of Organic Compounds*, pp. 123–131, 219–262, Wiley & Sons, New York (1991).
[34] P.S. Kalsi. *Spectroscopy of Organic Compounds*, pp. 206–210, 246–256, 342–350, New Age International Ltd, New Delhi, India (2005).
[35] J.M. Miller, K. Balasanmugam. *Can. J. Chem.*, **67**, 1496 (1989).
[36] N.G. Tsierkezos, U. Ritter, A.I. Philippopoulos, D. Schroder. *J. Coord. Chem.*, **63**, 3517 (2010).
[37] E. Alessio, G. Mestroni, G. Balducci, W.M. Attia, C.G. Calligaris. *Inorg. Chem.*, **30**, 609 (1991).
[38] K.D. Keerthi, B.K. Santra, G.K. Lahiri. *Polyhedron*, **17**, 1387 (1998).
[39] U.C. Sarma, R.K. Poddar. *Polyhedron*, **7**, 1737 (1988).
[40] A.B.P. Lever. *Inorganic Electronic Spectroscopy*, Elsevier, Amsterdam, The Netherlands (1984).
[41] S. Dutta, P.K. Bhattacharya. *Ind. J. Chem.*, **42A**, 262 (2003).
[42] R.S. Srivastava, F.R. Fronezek, L.M. Romero. *Inorg. Chim. Acta*, **357**, 2410 (2004).
[43] T. Bora, M.M. Singh. *J. Inorg. Nucl. Chem.*, **38**, 1815 (1976).

[44] W.L. Reynolds. *Prog. Inorg. Chem.*, **12**, 1 (1970).
[45] J.A. Davis. *Adv. Inorg. Chem. Radiochem.*, **24**, 115 (1981).
[46] E. Alessio. *Chem. Rev.*, **104**, 4203 (2004).
[47] P.K.L. Chan, B.R. James, D.C. Frost, P.K.H. Chan, H.L. Hu, K.A. Skov. *Can. J. Chem.*, **67**, 508 (1989).
[48] F.D. Rochon, P.C. Kong, L. Girard. *Can. J. Chem.*, **64**, 1897 (1986).
[49] J.D. Fortheringham, G.A. Heath, A.J. Lindsay, T.A. Stephensen. *J. Chem. Res. Miniprint*, **82**, 801 (1986).
[50] J.D. Oliver, D.P. Riley. *Inorg. Chem.*, **23**, 156 (1984).
[51] P.E.B. Nicolas, O. Zava, J. Furrer, J.P. Dayson, B. Therrien. *Dalton Trans.*, **39**, 5272 (2010).
[52] S.N. Shukla, P. Gaur, R. Mehrotra, M. Prasad, H. Kaur, M. Prasad, R.S. Srivastava. *J. Coord. Chem.*, **62**, 2556 (2009).